

# RSC Advances



This is an *Accepted Manuscript*, which has been through the Royal Society of Chemistry peer review process and has been accepted for publication.

*Accepted Manuscripts* are published online shortly after acceptance, before technical editing, formatting and proof reading. Using this free service, authors can make their results available to the community, in citable form, before we publish the edited article. This *Accepted Manuscript* will be replaced by the edited, formatted and paginated article as soon as this is available.

You can find more information about *Accepted Manuscripts* in the [Information for Authors](#).

Please note that technical editing may introduce minor changes to the text and/or graphics, which may alter content. The journal's standard [Terms & Conditions](#) and the [Ethical guidelines](#) still apply. In no event shall the Royal Society of Chemistry be held responsible for any errors or omissions in this *Accepted Manuscript* or any consequences arising from the use of any information it contains.

1 **Molecularly imprinted fluorescent chemosensor synthesized using**  
2 **quinoline-modified- $\beta$ -cyclodextrin as monomer for spermidine**  
3 **recognition**

4  
5 Yang Cheng<sup>a,b</sup>, Ping Jiang<sup>a</sup> and Xiangchao Dong<sup>a,b,\*</sup>  
6

7 <sup>a</sup> College of Chemistry, Nankai University, Tianjin 300071, China;

8 <sup>b</sup> Collaborative Innovation Center of Chemical Science and Engineering (Tianjin),  
9 Tianjin 300071, China;

10

11

12

13 **Abstract:**

14 Polyamines are polycationic amines and playing important functions in the cellular  
15 growth and proliferation. The abnormal levels of polyamines in the biological fluids  
16 have been related to different diseases including cancers. However, polyamine  
17 analysis is a difficult task because there are no chromophore in the polyamine  
18 structures. In this study, a novel molecularly imprinted fluorescent chemosensor for  
19 spermidine detection has been synthesized using quinoline modified- $\beta$ -cyclodextrin as  
20 the functional monomer. The imprinted receptors were formed by the interaction  
21 between the spermidine and  $\beta$ -cyclodextrin ( $\beta$ -CD). The fluorescence of the  
22 chemosensor has shown a “Turn-on” response mode which was resulted from the  
23 increase of the environmental hydrophobicity around quinoline group due to the  
24 inclusion of spermidine in the CD cavity. The chemosensor has selectivity for the  
25 spermidine and its structural analogue spermine due to the imprinting effect. In the  
26 research, the binding constant of the imprinted membrane was evaluated and binding  
27 mechanism of the MIP was studied by 2D <sup>1</sup>H NMR experiment. The research of  
28 spermidine analysis in serum demonstrated the imprinted chemosensor has good  
29 application potential in the biological sample analysis.

30

31 **Keywords:** molecularly imprinted chemosensor; spermidine; quinoline  
32 modified- $\beta$ -cyclodextrin; fluorescent detection

33

## 34 **1. Introduction**

35

36 The natural polyamines, including putrescine, spermidine and spermine, are  
37 polycationic amines produced in vivo metabolism. The significance of polyamines in  
38 cellular growth and proliferation is well recognized.<sup>1</sup> The important roles of  
39 polyamines in the stabilization of negative charges of DNA, RNA transcription,  
40 protein synthesis, and apoptosis have been studied. Research has found that increase  
41 in polyamines and polyamine synthesis enzymes are often related to the tumor  
42 growth.<sup>2</sup> The level of some polyamines can be indicative of the presence of malignant  
43 tumors, and was proposed as a tool for the cancer therapy effectiveness evaluations.<sup>3</sup>

44 Due to their multiple functions in cell biology, determination of the polyamines  
45 becomes an important task in the biological and pharmaceutical research. However,  
46 analysis of polyamines has been a challenge task because polyamines have neither  
47 chromophores and fluorophores nor the electrochemical activities. As the result, they  
48 cannot be readily analyzed by spectrophotometric or electrochemical methods.

49 Immunoassays (RIA and ELISA),<sup>4-6</sup> high performance liquid chromatography  
50 (HPLC)<sup>7, 8</sup> and thin layer chromatography (TLC)<sup>9</sup> have been used for the analysis of  
51 polyamines in serum or other body fluids. However, these methods have some  
52 drawbacks. For the immunoassay, the antibody is expensive and specificity is not  
53 satisfactory. The RIA may be hazardous due to its radioactivity. The HPLC and TLC  
54 methods for the polyamine analysis have to be coupled with derivatization  
55 experiment.<sup>10, 11</sup> While derivatization processes are time-consuming and interference  
56 compounds could be produced. Thus, it is desirable to develop a rapid, sensitive and  
57 selective method for the polyamine determination in biological samples.

58 Molecular imprinting is an effective technique for the preparation of molecularly  
59 imprinted polymers (MIPs). The imprinted binding sites in the MIPs can be created by  
60 the self-assembly of template molecule and functional monomers, followed by  
61 polymerization process.<sup>12, 13</sup> Due to the advantages such as tailor-made selectivity,

62 chemical stability and ease in preparation, MIPs have attracted great attention in the  
63 fields of chemical recognition and separations. They are also used as the alternative to  
64 biological receptors.<sup>14</sup> MIP fluorescent sensors have been synthesized and reported in  
65 the literature.<sup>15-17</sup> Among these researches, many reporting systems of the sensors  
66 relied on the fluorescence of analytes.<sup>18,19</sup> Some studies utilized electron transfer or  
67 formation of a resonance complex between the fluorescent monomer and analytes to  
68 switch on fluorophores.<sup>18,20</sup> These reporting systems are restricted to the analytes with  
69 specific structures. MIP fluorescent sensor with broader analyte application is  
70 desirable.

71 In the MIP preparations,  $\beta$ -cyclodextrin ( $\beta$ -CD) is an attractive monomer for  
72 organic compound recognition.  $\beta$ -CD has a hydrophobic inner cavity and hydrophilic  
73 outer surfaces. It is capable of interacting with a large variety of guest molecules to  
74 form inclusion complexes in aqueous environment.<sup>21-24</sup> With this property,  $\beta$ -CD has  
75 shown advantage in binding neutral molecules in the aqueous environment such as  
76 biological samples. Research of molecular imprinting using cyclodextrin (CD) as  
77 monomer has been published in the recognition of molecules such as bilirubin,<sup>25</sup>  
78 steroidal,<sup>26,27</sup> ursolic acid,<sup>28</sup> creatinine<sup>29,30</sup> and protein.<sup>31</sup> Using fluorophores labeled  
79 CD as acceptor for MIP fluorescent sensor have several advantages. It has good  
80 selectivity and is suitable for the application in the aqueous solutions. It has broader  
81 applications compared with some published work which has certain requirement for  
82 the structure of the analytes. We have used dansyl-modified  $\beta$ -cyclodextrin to  
83 synthesize the cholesterol imprinted chemosensor. The research demonstrated that  
84 fluorescent group-modified  $\beta$ -cyclodextrin can be used as building block for the  
85 imprinted receptor and attached fluorescent group can be used as the reporter.  
86 However, the dansyl-modified  $\beta$ -cyclodextrin MIP in our research exhibited a  
87 “Turn-off” response mode with low sensitivity which is the weakness for detection.<sup>32</sup>  
88 To construct a MIP fluorescent chemosensor with “Turn-on” mode is one of the goals  
89 in this research.

90 As far as we know, there is no research of MIP for polyamines analysis that has  
91 been published. This is the first research developed for the spermidine analysis by

92 using MIP as the acceptor of the fluorescence sensor. In this research, a new  
93 fluorescent imprinted chemosensor for the spermidine detection has been developed.  
94 A quinoline group derivatized  $\beta$ -CD was synthesized and employed as the functional  
95 monomer. The spermidine/ $\beta$ -CD interaction was used to form binding sites of MIP  
96 and the quinoline groups are acting as fluorescent reporter. Research has demonstrated  
97 that with certain sidearm, the quinoline group can co-exist with included guest  
98 molecule in the CD cavities.<sup>33</sup> The inclusion event increases the hydrophobicity of the  
99 cavity environment and results in an increase of the fluorescent intensity of the  
100 quinoline group.<sup>33</sup> This fluorescence “Turn-on” mechanism was employed in the  
101 present research to create a reporting system in the chemosensor. In the research, the  
102 sensitivity, selectivity and application of the chemosensor have been studied. The  
103 mechanism of imprinting was also investigated by 2D <sup>1</sup>H NMR experiment. The  
104 result demonstrated that the chemosensor synthesized in this study has rapid and  
105 selective response to the binding of the spermidine with a Tune-on mode.

106

## 107 **2. Materials and methods**

108

### 109 **2.1. Materials**

110

111 The  $\beta$ -cyclodextrin ( $\beta$ -CD) and tosyl chloride were purchased from Guangfu  
112 Chemical Co. Ltd. (Tianjin, China). Spermidine, 2-phenethylamine, spermine,  
113 8-hydroxyquinoline and hexamethylene diisocyanate (HMDI) were obtained from  
114 Tianjin Heowns Biochemical Technology Co. Ltd (Tianjin, China). *N*,  
115 *N'*-dimethylformamide (DMF) and dimethyl sulfoxide (DMSO) were from Kermel  
116 Chemical Co. Ltd. (Tianjin, China) and were dried with molecular sieve and distilled  
117 under a reduced pressure before use. All other reagents were of analytical grade and  
118 used as received. Serum was from Huyu Biochemical Technology Co. Ltd (Shanghai,  
119 China) and stored at -20 °C until use.

120

### 121 **2.2. Instrumentation**

122

123 Elemental analyses were carried out with an elemental analyzer (Vario EL CUBE,  
124 Germany). A TU-1901 spectrophotometer (Purkinje, China) was used for the UV  
125 measurement.  $^1\text{H}$  NMR experiments were performed on a Mercury Vx-300  
126 spectrometer (Varian, USA). Fluorescence spectra were obtained from a Hitachi-4500  
127 fluorescence spectrometer (Hitachi, Japan). FT-IR spectra were recorded on a Nicolet  
128 6700 FT-IR spectrophotometer (Nicolet, USA).

129

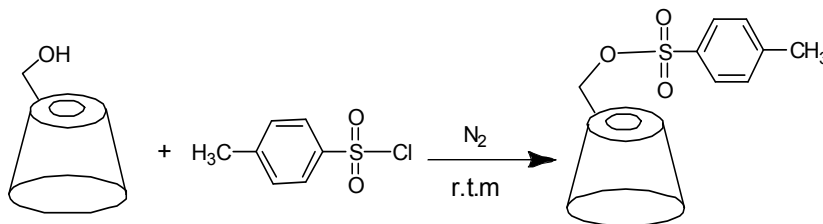
### 130 **2.3. Synthesis of 6-O-(p-tosyl)- $\beta$ -cyclodextrin**

131

132 The 6-O-(p-tosyl)- $\beta$ -cyclodextrin ( $\beta$ -CDOTS) was synthesized by the reaction of  
133  $\beta$ -CD and tosyl chloride (Fig. 1) according to the method in the literature.<sup>34</sup>  $\beta$ -CD  
134 (11.2 g, 9.9 mmol) was dissolved in 112 mL dry pyridine. Tosyl chloride (3.75 g, 19.7  
135 mmol) was dissolved in 12 mL of dry pyridine and added drop-wise into  $\beta$ -CD  
136 solution under nitrogen protection. The reaction was performed under stirring for 7 h  
137 at room temperature. After the reaction, the solution was poured into 400 mL of  
138 acetone. The white precipitates were collected and washed with acetone. The product:  
139  $\beta$ -CDOTS was purified by three successive re-crystallizations in water and dried in  
140 vacuum at 60 °C.

141  $^1\text{H}$  NMR (300 MHz,  $\text{D}_6$ -DMSO):  $\delta$  2.42 (3H, s, -CH<sub>3</sub>), 3.18~3.42 (14H, m,  
142 C2-H, C4-H), 3.43~3.74 (28H, m, C3-H, C5-H, C6a, C6b-H), 4.13~4.55 (6H, m,  
143 C6-OH), 4.76~4.82 (7H, s, C1-H), 5.58~5.87 (14H, m, C2-OH, C3-OH), 7.40~  
144 7.45 (2H, d, J=15 Hz, Ph-H), 7.72~7.77 (2H, d, J=15 Hz, Ph-H). The results of  
145 elemental analysis for the product were: C, 43.56; H, 6.18, which agreed with the  
146 values of  $\beta$ -CDOTS $\cdot$ 3H<sub>2</sub>O molecule (C<sub>49</sub>H<sub>76</sub>O<sub>37</sub>S $\cdot$ 3H<sub>2</sub>O). The FT-IR experiment was  
147 also carried on to characterize the  $\beta$ -CDOTS (Fig. S1 in the Supporting Information).  
148 The results have shown that the tosyl ester was successfully grafted on  $\beta$ -CD.

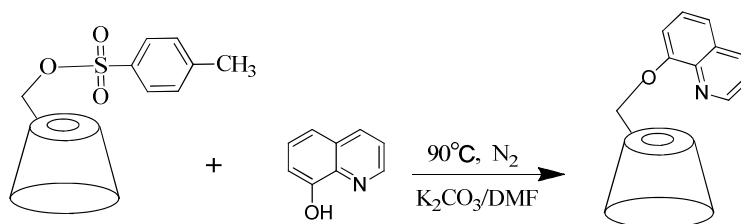
149



150  
151 **Fig. 1.** Synthesis of 6-O-(p-tosyl)-β-CD (β-CDOTS).  
152

153 **2.4. Synthesis of mono [6-O-(8-quinolyl)]-β-cyclodextrin**  
154

155 The mono [6-O-(8-quinolyl)]-β-cyclodextrin (quinolyl-β-CD) was synthesized  
156 by the reaction of β-CDOTS and 8-hydroxyquinoline (Fig. 2) according to a  
157 literature.<sup>35</sup> In the reaction, β-CDOTS (2 g) and 8-hydroxyquinoline (1 g) were  
158 dissolved in 30 mL DMF. After addition of potassium carbonate (0.3 g), the reaction  
159 was performed at 90 °C for 20 h under a nitrogen atmosphere and stirring. The yellow  
160 precipitates were obtained after removal of the solvents under a reduced pressure at  
161 40 °C. The product was dried at 60 °C under vacuum for 8 h and was purified by  
162 recrystallization in water. <sup>1</sup>H NMR (DMSO-d<sub>6</sub>, TMS): δ 3.2 - 4.3 (m, β-cyclodextrin  
163 protons); 7.1 - 9.2 (m, 8-quinolyl protons); Anal. Calcd for C<sub>51</sub>H<sub>75</sub>O<sub>35</sub> N·6H<sub>2</sub>O: C,  
164 44.70; H, 6.30; N, 1.02. Found: C, 44.41; H, 5.93; N, 1.08. The FT-IR (Fig. S1 in the  
165 Supporting Information) also indicated the successful grafting of the quinolyl group  
166 on β-CD.



168  
169 **Fig. 2.** Synthesis of mono [6-O-(8-quinolyl)]-β-cyclodextrin (quinolyl-β-CD).  
170

171 **2.5. Preparation of spermidine fluorescent imprinted membrane**  
172

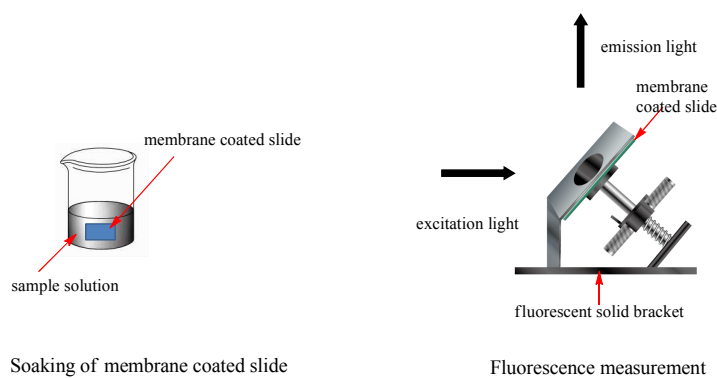
173 In the MIP membrane preparation, spermidine was used as the template and  
174 quinoyl- $\beta$ -CD was the functional monomer. HMDI was used as the cross-linker. The  
175 quinoyl- $\beta$ -CD (0.2 g), spermidine (11.5  $\mu$ L) and HMDI (0.15 mL) were dissolved in  
176 3 mL of dry DMSO under stirring. The pre-polymerization solution was spread onto a  
177 clean glass slide (38 mm $\times$ 20 mm) by the doctor blade coating technique. The MIP  
178 membrane was formed on the slide by polymerization at 65  $^{\circ}$ C for 2 h. The membrane  
179 coated slide was washed with acetone, hot water and ethanol consecutively to remove  
180 the template molecules and reagent residues under ultrasonication and then dried  
181 under vacuum at 40  $^{\circ}$ C for 2 h. As a control, a non-imprinted membrane was prepared  
182 under the same conditions except the template molecules are omitted.

183

## 184 2.6. Fluorescence spectra measurement and binding constant determination

185

186 Spermidine standard solutions with different concentrations were prepared with  
187 deionized water and stored in refrigerator before use. The membrane coated slide was  
188 soaked in spermidine solution for 4 min and was amounted in the specialized solid  
189 bracket supplied by Hitachi for the measurement. A 2.5 nm slit and photomultiplier  
190 tube voltage of 700 V were employed in the experiment. Fluorescence spectra of the  
191 chemosensor were obtained at  $\lambda_{\text{ex}}$  of 324 nm and  $\lambda_{\text{em}}$  of 411 nm at room temperature.  
192 The method of the soaking of the membrane and fluorescence measurement was  
193 demonstrated in Fig. 3.



194

195 **Fig. 3.** Schematic representation for the sample soaking and fluorescence  
196 measurement.



197

198 The binding constant of the spermidine on the imprinted membrane and  
199 non-imprinted membrane were determined by modified double reciprocal plot  
200 equation.<sup>36</sup>

$$201 \quad 1/\Delta I = (K k Q_{\text{com}} C_{\text{m}})^{-1} C_{\text{s}}^{-1} + (k Q_{\text{com}} C_{\text{m}})^{-1} \quad (\text{Eq. 1})$$

202 In the equation,  $\Delta I$  is the fluorescence intensity difference between the blank and  
203 the analyte-bound chemosensor,  $K$  is the binding constant,  $k$  is the instrumental  
204 constant,  $Q_{\text{com}}$  is the quantum yield of complex,  $C_{\text{m}}$  is the concentration of the binding  
205 sites of the imprinted membrane,  $C_{\text{s}}$  is the concentration of spermidine. The  $k Q_{\text{com}} C_{\text{m}}$   
206 are constants in the experiment and the product of  $k Q_{\text{com}} C_{\text{m}}$  can be obtained from the  
207 intercept of the plot. The binding constant was calculated by dividing the intercept  
208 with the slope of the plot.

209

## 210 **2.7. 2D <sup>1</sup>H NMR experiment for the determination of quinoyl-β-CD/spermidine** 211 **complex structure**

212

213 2D <sup>1</sup>H NMR experiments were performed on a Mercury Vx-300 spectrometer  
214 (Varian, USA). The sample was prepared by dissolving quinoyl-β-CD and spermidine  
215 in d<sub>6</sub>-DMSO. The ratio of quinoyl-β-CD/spermidine in solution was the same as that  
216 used in the imprinting polymerization. 2D <sup>1</sup>H NMR ROESY was performed at a  
217 spectral width of 4807 Hz in both dimensions and 512 increments with 64 transients  
218 per increment. The mixing time was 240 ms.

219

## 220 **2.8. Determination of spermidine in the spiked serum samples**

221

222 The spermidine standard solution ( $1 \times 10^{-4}$  mol·L<sup>-1</sup>) was prepared in deionized  
223 water. Spiked serum samples with different spermidine concentrations were prepared  
224 by mixing different volumes (30, 60, 185, 315, 666 μL) of the spermidine standard  
225 solution with 1.0 mL serum under vortexing. To remove proteins from the serum  
226 samples, 2.0 mL deionized water and 3.0 mL acetonitrile were added into the samples  
227 followed by centrifugation at 8000 rpm for 10 min. The supernatant was used for the  
228 fluorescence analysis. The sample soaking time and conditions for the fluorescence

229 measurement were the same as section 2.6.

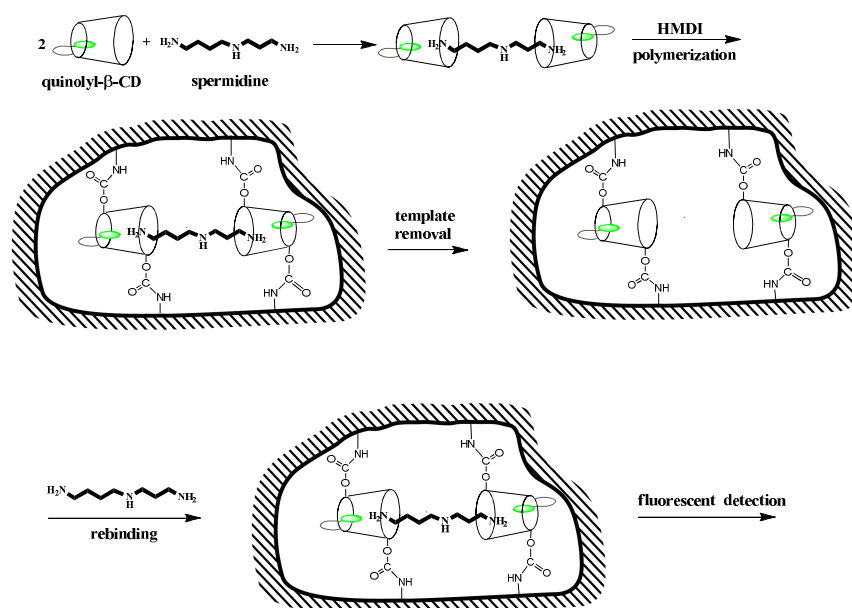
230

### 231 **3. Results and Discussion**


232

#### 233 **3.1. Imprinting and proposed signaling mechanism of the molecularly imprinted** 234 **fluorescent chemosensor**

235 In the present study, a molecularly imprinted membrane was synthesized as the  
236 accepting and reporting system of a fluorescent chemosensor. The artificial receptor  
237 was created by molecular imprinting using quinoly- $\beta$ -CD as the functional monomer.  
238 The synthesis of the spermidine imprinted binding sites and proposed sensing  
239 mechanism are demonstrated in the Fig. 4. In the quinoly- $\beta$ -CD molecule synthesized  
240 in this research, the quinoline group is self-included in the cavity of  $\beta$ -CD before  
241 interaction with guest molecules, which has been proved by 2D  $^1\text{H}$  NMR  
242 experiment.<sup>33</sup> We proposed that in the imprinting process, spermidine is encapsulated  
243 within the quinoly- $\beta$ -CD. The complex structures were fixed in the MIP by  
244 polymerization. After the MIP synthesis, the template is removed from the MIP by  
245 washing process, which leaves only the quinoline groups in the  $\beta$ -CD cavity. In the  
246 rebinding process, spermidine re-enters the  $\beta$ -CD and co-exists with quinoline group  
247 in the cavities. The existing of spermidine in  $\beta$ -CD makes the environment  
248 surrounding the quinoline group more hydrophobic, which induces an increase of the  
249 fluorescence intensity. The fluorescent intensity change of the quinoline group signals  
250 the binding event.



251

252 **Fig. 4.** Schematic demonstration of molecular imprinting for the receptor construction  
 253 and re-binding of spermidine giving fluorescence signal.  = quinoline  
 254 group.

255

### 256 3.2. Selection of the synthetic condition for imprinted membrane

257

258 In the MIP synthesis, the ratio of template/functional monomer/cross-linker has  
 259 to be selected. To find a proper functional monomer/template ratio, complexation  
 260 stoichiometry of quinolyl-β-CD/spermidine was studied by the Job's plot method. In  
 261 the experiment, the ratios of the quinolyl-β-CD and spermidine were changed while  
 262 the total concentrations of quinolyl-β-CD and spermidine in the solutions were kept  
 263 constant. The difference of UV absorbance ( $\Delta A$ ) between solutions of mixture and  
 264 quinolyl-β-CD were measured. The complexation stoichiometric ratio of the  
 265 quinolyl-β-CD and spermidine was determined through Job's plot (Fig. S2 in the  
 266 Supporting Information). In the Job's plot, the maximum  $\Delta A$  appeared when the  
 267 quinolyl-β-CD/spermidine ratio was 1.5. The quinolyl-β-CD/spermidine ratio of 2:1  
 268 was selected in the imprinted membrane synthesis to make the incorporation reaction  
 269 more completed.

270

The ratio of 1:6 was selected for the functional monomer/cross-linker, which was

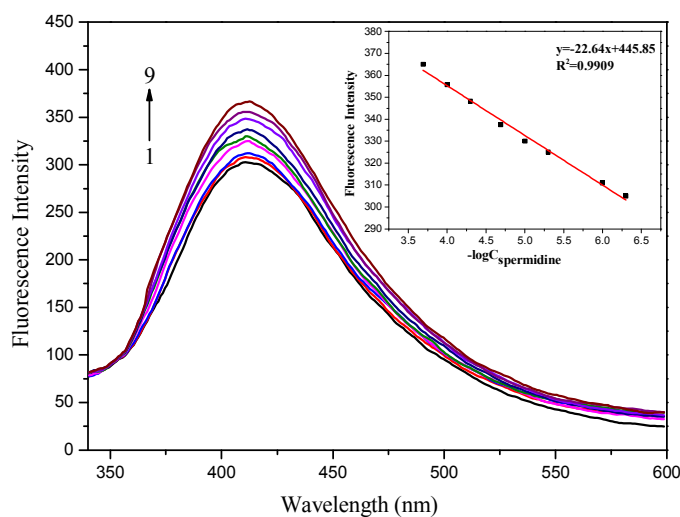
271 the optimized composition from our previous research experiment.<sup>32</sup>

272

### 273 3.3. The fluorescent response and binding affinity of the imprinted fluorescent 274 chemosensor

275

276 The optical response of the spermidine-imprinted chemosensor upon binding of  
277 spermidine was studied by the fluorescent experiment. The fluorescence spectra of the  
278 chemosensor after soaking in spermidine solutions with different concentrations are  
279 shown in the Fig. 5. The fluorescence intensity of the chemosensor increased with the  
280 increase of the spermidine concentration. This “Turn on” response mode indicated the  
281 cavities of the imprinted  $\beta$ -CD accommodate both the quinoline groups and  
282 spermidine molecules. This phenomenon agreed with our proposed binding  
283 mechanism (Fig. 4). A linear relation between the negative logarithm of spermidine  
284 concentration ( $-\log C_{\text{spermidine}}$ ) and fluorescence intensity of the chemosensor at  
285  $C_{\text{concentration}}$  of  $5 \times 10^{-7}$  to  $2 \times 10^{-4} \text{ mol}\cdot\text{L}^{-1}$  has been obtained.

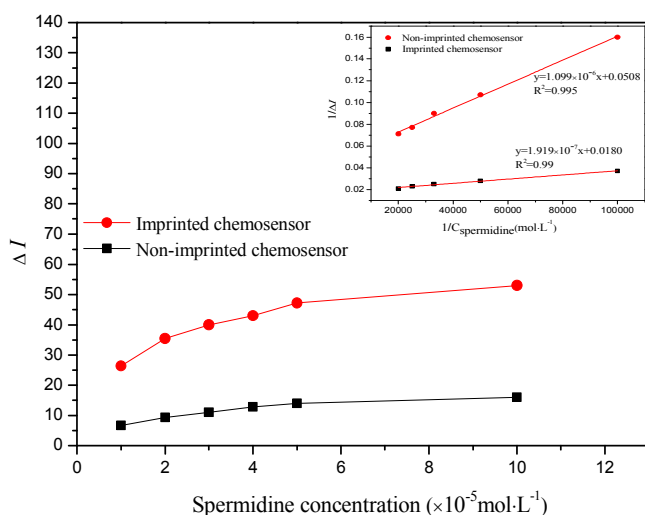


286 **Fig. 5.** Fluorescence spectra of imprinted membrane upon soaking of spermidine  
287 solutions with different concentrations at room temperature. The  
288 concentrations of spermidine were (from 1 to 9)  $0, 5 \times 10^{-7}, 1 \times 10^{-6}, 5 \times 10^{-6},$   
289  $1 \times 10^{-5}, 2 \times 10^{-5}, 5 \times 10^{-5}, 1 \times 10^{-4}, 2 \times 10^{-4} \text{ mol}\cdot\text{L}^{-1}$ .

290 The binding kinetic of the imprinted membrane was determined by the  
291 measurement of the response of the imprinted chemosensor for spermidine versus the  
292 sample soaking time (Fig. S3 in the Supporting Information). The spermidine H<sub>2</sub>O  
293 solution with concentration of  $1.0 \times 10^{-5} \text{ mol} \cdot \text{L}^{-1}$  was used in the experiment. The result  
294 demonstrated the binding equilibrium was reached at 4 min. The fluorescence  
295 measurements were performed after sample soaking for 4 min.

296 To study the imprinted binding affinity of the imprinted membrane, the binding  
297 constant was calculated by modified double reciprocal plot equation (Eq. 1). The plot  
298 of  $\Delta I$  versus spermidine concentrations in the range from  $1 \times 10^{-5}$  to  $10 \times 10^{-5} \text{ mol} \cdot \text{L}^{-1}$   
299 for imprinted and non-imprinted membranes are shown in the Fig. 6.  $\Delta I$  is the  
300 fluorescence intensity difference between the blank and the analyte-bound  
301 chemosensor.

302 The result demonstrated that the imprinted chemosensor has higher fluorescence  
303 response and sensitivity than the non-imprinted chemosensor. The data from  
304 spermidine concentrations in the range from  $1 \times 10^{-5}$  to  $5 \times 10^{-5} \text{ mol} \cdot \text{L}^{-1}$  were used for  
305 the binding constant calculation. The binding constant  $K_{\text{MIP}}$  of the spermidine on the  
306 imprinted membrane is  $9.4 \times 10^4 \text{ L} \cdot \text{mol}^{-1}$  and it ( $K_{\text{NIP}}$ ) is  $4.6 \times 10^4 \text{ L} \cdot \text{mol}^{-1}$  for the  
307 non-imprinted membrane. The higher binding constant was contributed to the specific  
308 binding cavity created in the imprinted process which enhanced the binding affinity  
309 for the template. The imprinted factor, calculated by  $K_{\text{MIP}}/K_{\text{NIP}}$  was 2.04, which  
310 indicated that good imprinting effect was obtained.



311  
 312 **Fig. 6.** Sensitivity comparison of imprinted chemosensor with non-imprinted  
 313 chemosensor in six different concentrations of spermidine ( $1 \times 10^{-5}$ ,  
 314  $2 \times 10^{-5}$ ,  $3 \times 10^{-5}$ ,  $4 \times 10^{-5}$ ,  $5 \times 10^{-5}$  and  $10 \times 10^{-5} \text{ mol}\cdot\text{L}^{-1}$ ).  
 315

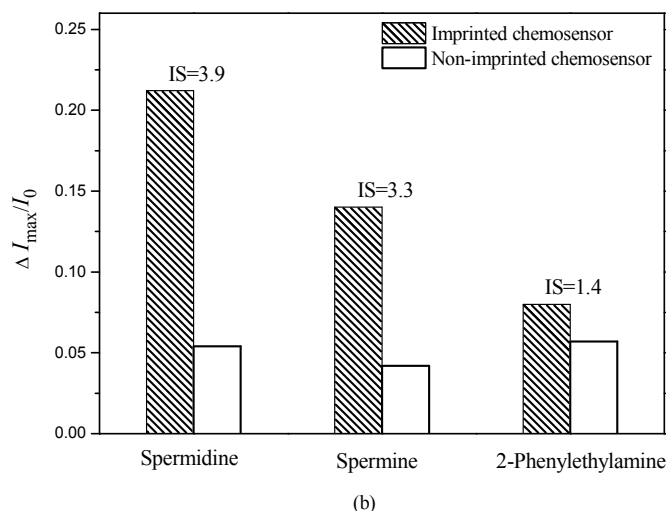
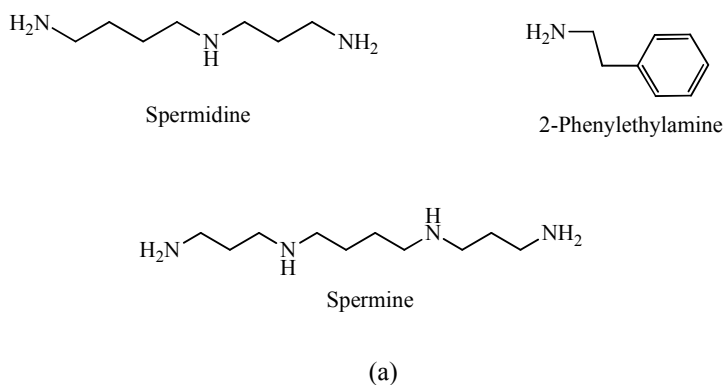
### 316 3.4. Selectivity of the spermidine imprinted chemosensor

317  
 318 The selectivity of the spermidine imprinted chemosensor was evaluated by  
 319 comparison of the imprinted membrane sensitivity for spermidine and for its analogs.  
 320 The structures of the analytes used in the selectivity study are shown in the Fig. 7 (a).

321 The sensitivity factor of the membrane for spermidine  $S_f$  was calculated by  
 322  $S_f = \Delta I_{max} / I_0$ , in which  $I_0$  is the fluorescence intensity of the blank imprinted membrane  
 323 and  $\Delta I_{max}$  is the maximum fluorescence intensity difference between the blank and the  
 324 analyte-bound chemosensor. The sensitivity factors of imprinted chemosensor and  
 325 non-imprinted chemosensor for three analytes are shown in the Fig. 7 (b). The  
 326 sensitivity of the imprinted chemosensor for different analytes is in the order of  
 327 spermidine > spermine > 2-phenylethylamine. While for the non-imprinted  
 328 chemosensor, the sensitivity is 2-phenylethylamine > spermidine > spermine. The  
 329 imprinted selectivity (IS) of the MIP calculated by  $S_f(\text{MIP}) / S_f(\text{NIP})$  are shown in the  
 330 Fig. 7 (b). The different order of sensitivity between the imprinted and non-imprinted  
 331 chemosensors proved that the selectivity of the chemosensor comes from the  
 332 imprinting process. The IS of 3.9 for spermidine demonstrated that good recognition  
 333 was obtained due to the imprinting process. The selectivity ( $\alpha$ ) of the chemosensor

334 was evaluated by the ratio of sensitivity of spermidine to its analogs,  
335  $\alpha = S_f(\text{spermidine})/S_f(\text{analog})$ . The  $\alpha(\text{spermidine}/2\text{-phenylethylamine})$  was 2.65 and  
336  $\alpha(\text{spermidine}/\text{spermine})$  was 1.5 for the imprinted chemosensor, while they were 0.94  
337 and 1.28 for the non-imprinted chemosensor respectively. The results indicated that  
338 the imprinted chemosensor has good selectivity for imprinted molecule than its  
339 analogs and the selectivity is much better than the non-imprinted chemosensor.

340



341

342 **Fig. 7.** Comparison of fluorescent sensitivity of imprinted and non-imprinted  
343 chemosensor. (a) Chemical structures of the analytes used in the selectivity  
344 study; (b) fluorescent sensitivity of imprinted and non-imprinted  
345 chemosensors for three analytes. The concentration of the analytes was  
346  $2 \times 10^{-4} \text{ mol} \cdot \text{L}^{-1}$ . The excitation wavelength was 324 nm and the emission  
347 wavelength was 411 nm.

### 348 3.5. The 2D $^1\text{H}$ NMR analysis of the quinolyl- $\beta$ -CD/spermidine complex structure

349

350 To explore the imprinting mechanism, we studied the quinolyl- $\beta$ -CD/spermidine  
351 (Fig. 8 (a)) complex structure by 2D  $^1\text{H}$  NMR experiment. The ROESY spectrum of  
352 quinolyl- $\beta$ -CD/spermidine complex is shown in the Fig. 8 (b). The assignment for the  
353 cross-peaks with correlated protons is listed in the Table 1. In the 2D  $^1\text{H}$  NMR  
354 spectrum, ROESY cross-peak A from the correlation between  $\beta$ -CD proton ( $\text{H}_6$ ) and  
355 quinoline proton ( $\text{H}_e$ ) was observed (Table 1), which indicated that quinoline is  
356 self-included into the  $\beta$ -CD cavity. Meanwhile, as shown in Fig. 8 (b), several  
357 cross-peaks between quinolyl- $\beta$ -CD and spermidine protons appeared in the 2D  $^1\text{H}$   
358 NMR spectrum, suggesting that the spermidine molecule exists in the cavity of  
359 quinolyl- $\beta$ -CD.

360 The ROESY cross peaks B, C and D are the correlation signals between the  $\text{C}_1$ -H  
361 (and  $\text{C}_7$ -H),  $\text{C}_6$ -H,  $\text{C}_2$ -H of spermidine and the protons  $\text{H}_3$ ,  $\text{H}_3$ ,  $\text{H}_5$  of  $\beta$ -CD,  
362 respectively (Table 1). These correlation signals demonstrated the distance between  
363 the two protons is within 0.5 nm. This result indicated that spermidine is included into  
364 the cavity of quinolyl- $\beta$ -CD.

365 The correlation signals between other inner cavity proton  $\text{H}_5$  and any quinoline  
366 protons are not observed, which excluded the possibility of the quinoline group in the  
367 central cavity. All information reveals that the spermidine is included into the  $\beta$ -CD  
368 cavity from its secondary side. Fig. 8 (c) shows the possible complex structure of  
369 quinolyl- $\beta$ -CD/spermidine.

370 For comparison, quinolyl- $\beta$ -CD structure was also studied by 2D  $^1\text{H}$  NMR  
371 experiment (Fig. S4 in the Supporting Information), ROESY cross-peak A' between  
372 the  $\beta$ -CD proton ( $\text{H}_6$ ) and the quinoline proton ( $\text{H}_e$ ) was also observed, which has  
373 similar intensity as peak A in Fig. 8. This phenomenon indicates that the binding of  
374 the spermidine does not influence the position of the quinoline group in the cavity of  
375  $\beta$ -CD.

376

377



378 **Table 1** 2D  $^1\text{H}$  NMR ROESY cross-peaks between the protons of quinoline group,  
 379 spermidine and  $\beta$ -cyclodextrin.  
 380

Cross peak	Correlated protons	Intensity
A	$\beta$ -CD, H <sub>6</sub> H <sub>e</sub> of quinoline	+++
B	$\beta$ -CD, H <sub>3</sub> C1-H of spermidine C7-H of spermidine	+++ +++
C	$\beta$ -CD, H <sub>3</sub> C6-H of spermidine	++
D	$\beta$ -CD, H <sub>5</sub> C2-H of spermidine	+

381

382

383

384

385

386

387

388

389

390

391

392

393

394

395

396

397

398

399

400

401

402

403

404

405

406

407

408

409

410

411

412

413

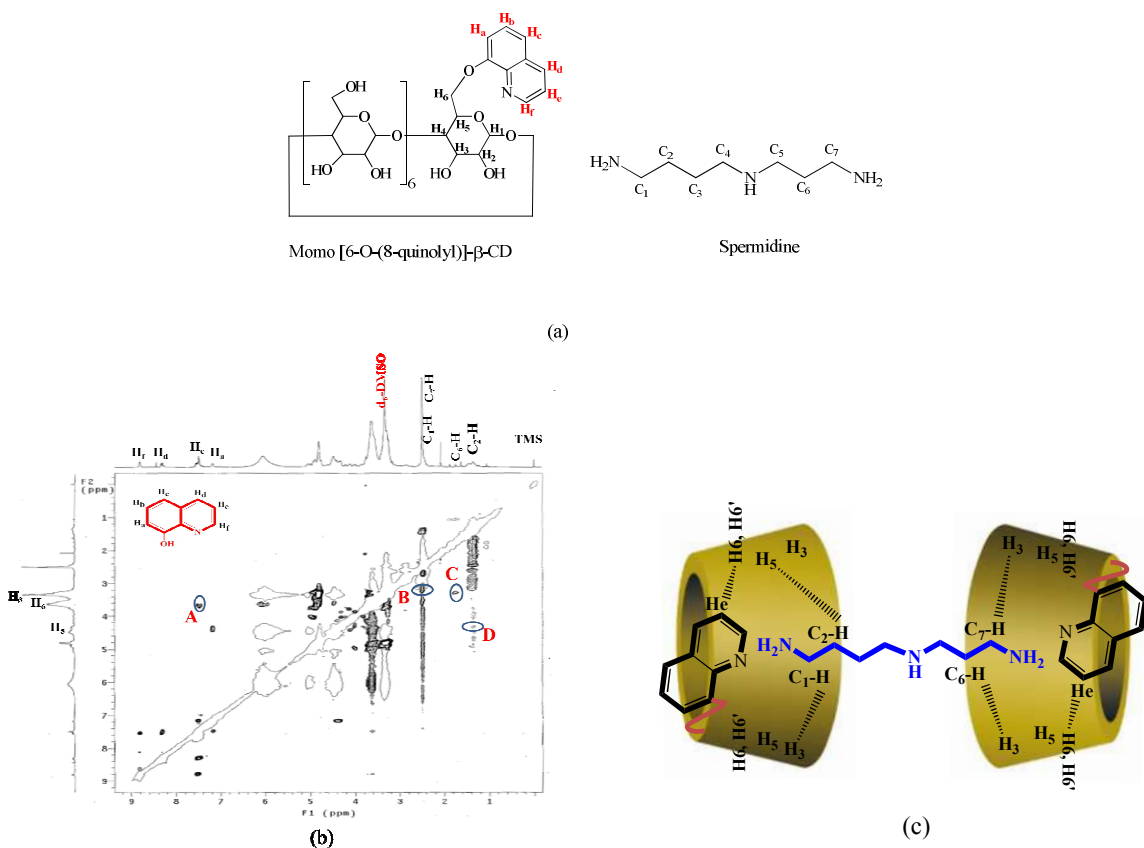


**Fig. 8.** 2D  $^1\text{H}$  NMR ROESY analysis of quinolyl- $\beta$ -CD/spermidine complex.

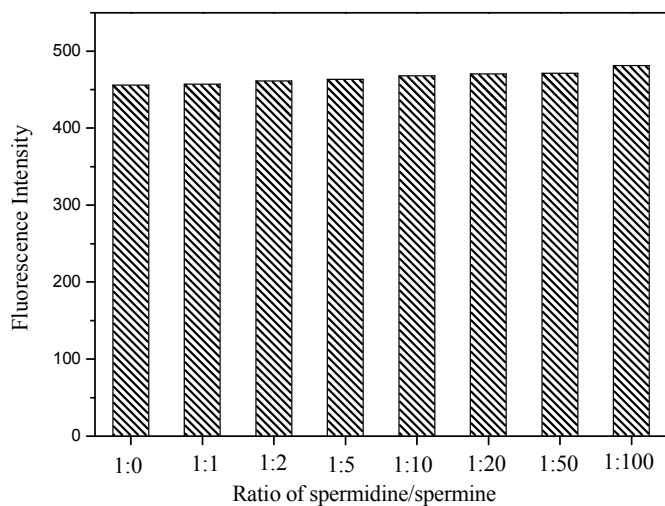
(a) Structures of mono [6-O-(8-quinolyl)]- $\beta$ -cyclodextrin and spermidine with labelled protons or carbons; (b) 2D  $^1\text{H}$  NMR ROESY spectrum of quinolyl- $\beta$ -CD/spermidine complex; (c) proposed quinolyl- $\beta$ -CD/spermidine complex structure.

### 414 3.6. Interference study

415

416 To further investigate the selectivity of the chemosensor, interference study was  
417 carried out using spermine as the interference component. The spermine has similar  
418 structure with spermidine and also exists in the biological fluids. The fluorescence  
419 response of mixture solutions with spermidine/spermine molar ratios of 1:1, 1:2, 1:5,  
420 1:10, 1:20, 1:50 and 1:100 were investigated using the MIP chemosensor. In the  
421 experiment, the spermidine concentration ( $1 \times 10^{-6} \text{ mol} \cdot \text{L}^{-1}$ ) was kept constant.

422 The fluorescence intensity versus different ratios of spermidine/spermine is  
423 shown in the Fig. 9. The results indicated that in the spermidine/spermine ratios from  
424 1:1 to 1:50, the increment of the fluorescence intensity was only 1% to 3%. When the  
425 ratio of spermine increased to 100:1, the increment of the fluorescence intensity was  
426 changed to 5.5%. Because the concentration of spermine in serum is generally lower  
427 than spermidine,<sup>8</sup> this situation rarely exist in the real samples. The result of  
428 interference study indicated that spermine does not have obvious influence for the  
429 spermidine determination.



430

431 **Fig. 9.** Fluorescence intensity of imprinted chemosensor in different ratios of  
432 spermidine/spermine.

433

434 **3.7. Determination of spermidine in serum using the imprinted chemosensor**

435

436 The study of spermidine determination in serum by fluorescence spectroscopy  
 437 was conducted to investigate the potential application of the imprinted chemosensor  
 438 in the biological sample analysis. The linearity of the quantification method was  
 439 determined by spermidine standard solution. A linear relation ( $y = -9.82x + 266.94$ )  
 440 between the fluorescence intensity and  $-\log C_{\text{spermidine}}$  in the spermidine concentration  
 441 range of  $1 \times 10^{-7}$  to  $2 \times 10^{-4}$  mol·L<sup>-1</sup> was established ( $R^2 = 0.9915$ ).

442 The accuracy and precision of the method were determined by the recovery and  
 443 RSD from the measurement of the spiked serum samples (Table 2). The spermidine in  
 444 the blank serum was  $1.25 \times 10^{-6}$  mol·L<sup>-1</sup> determined by imprinted chemosensor, which  
 445 closed to the analytical result in the literature.<sup>8, 37</sup> The recoveries measured by the  
 446 spiked spermidine samples were in the range of 88.0 % - 105.0 %, and the relative  
 447 standard deviation (RSD%) was less than 5%. The results demonstrated the  
 448 chemosensor system has good application potential for the detection of spermidine in  
 449 serum.

450 **Table 2** Determination of spermidine in the spiked serum using imprinted fluorescent  
 451 chemosensor (n=5).

452

Spiked Concentration (mol·L <sup>-1</sup> , × 10 <sup>-6</sup> )	Found Concentration (mol·L <sup>-1</sup> , × 10 <sup>-6</sup> )	Recovery (%)	RSD (%)
0.5	0.45	90.0	3.5
1	0.88	88.0	4.3
3	2.81	93.6	4.2
5	5.25	105.0	3.9
10	9.25	92.5	3.9

453

454 The comparison of different methods for the spermidine analysis was shown in the

455 Table 3. Compared with other methods, the method of this work has advantages of  
 456 short analytical time and simple sample pretreatment (no derivatization requirement).  
 457 It also has acceptable accuracy and linear range.

458

459 Table 3 Comparison of different methods for spermidine analysis in biological samples<sup>a</sup>

460

Methods	Pretreatment	Time of analysis	Linear range ( $\mu\text{ mol}\cdot\text{L}^{-1}$ )	Accuracy (Recovery, %)	Applied samples
HPLC-UV	derivatization	25 min	0.27-1.6	92-107	serum <sup>8</sup>
LC-MS	derivatization	12 min	0.007-1.7	84-108	serum <sup>37</sup>
Capillary electrophoresis	derivatization	10 min	0.01-1	93.4-102	urine <sup>38</sup>
RIA	-	60-80 samples/day	0.07-0.41	95-107	Serum <sup>39</sup>
Spermidine imprinted Chemosensor	-	4 min	0.1-200	88-105	serum (This work)

461 <sup>a</sup> “-” represents no derivatization in the pretreatment.

462

463

#### 464 4. Conclusion

465

466 A new spermidine imprinted fluorescent chemosensor was prepared by molecular  
 467 imprinting using quinoline modified- $\beta$ -cyclodextrin as the functional monomer. The  
 468 imprinted chemosensor has “Turn-on” response upon the addition of the template  
 469 molecules, which has better sensitivity. The imprinted fluorescent chemosensor has  
 470 selectivity to spermidine, which demonstrated that the imprinted cavities have been  
 471 successfully established. The proposed interaction mechanism between spermidine  
 472 and quinoline modified- $\beta$ -cyclodextrin has been proved by 2D <sup>1</sup>H NMR experiment.  
 473 The method using imprinted fluorescence chemosensor has been developed for the  
 474 detection of spermidine in serum sample with acceptable accuracy and precision. The  
 475 method also has short analytical time and good selectivity for spermidine, which

476 demonstrated the chemosensor has application potential for real sample analysis.

477

## 478 Acknowledgments

479

480 This work was supported by the National Natural Science Foundation of China (Grant  
481 No. 21375065) and State Key Laboratory of Chemo/Biosensing and Chemometrics,  
482 Hunan University.

483

484

485

486

487

488

## 489 References

490

- 491 1. D. Teti, M. Visalli and H. McNair, *J. Chromatogr. B*, 2002, **781**, 107-149.
- 492 2. M. H. Park and K. Igarashi, *Biomol. Ther.*, 2013, **21**, 1-9.
- 493 3. Z. Köstereli and K. Severin, *Chem. Commun.*, 2012, **48**, 5841-5843.
- 494 4. I. Garthwaite, A. D. Stead and C. C. Rider, *J. Immunol. Methods*, 1993, **162**, 175-178.
- 495 5. F. Bartos, D. Bartos, A. Dolney, D. Grettie and R. Campbell, *Res. Commun. Chem. Path. Phar.*,  
496 1978, **19**, 295-309.
- 497 6. N. Seiler and F. Raul, *J. Cell. Mol. Med.*, 2005, **9**, 623-642.
- 498 7. C. Molins-Legua, P. Campins-Falco, A. Sevillano-Cabeza and M. Pedron-Pons, *Analyst*, 1999,  
499 **124**, 477-482.
- 500 8. H.-m. Mao, B.-g. Chen, X.-m. Qian and Z. Liu, *Microchem. J.*, 2009, **91**, 176-180.
- 501 9. R. Jeya Shakila, T. Vasundhara and K. Kumudavally, *Food Chem.*, 2001, **75**, 255-259.
- 502 10. J. Lapa-Guimarães and J. Pickkova, *J. Chromatogr. A*, 2004, **1045**, 223-232.
- 503 11. A. Shalaby, *Food Chem.*, 1994, **49**, 305-310.
- 504 12. G. Wulff, *Angew. Chem. Int. Ed. Engl.*, 1995, **34**, 1812-1832.
- 505 13. K. Haupt and K. Mosbach, *Chem. Rev.*, 2000, **100**, 2495-2504.
- 506 14. C. Alexander, H. S. Andersson, L. I. Andersson, R. J. Ansell, N. Kirsch, I. A. Nicholls, J.  
507 O'Mahony and M. J. Whitcombe, *J. Mol. Recognit.*, 2006, **19**, 106-180.
- 508 15. R. J. Krupadam, B. Bhagat, S. R. Wate, G. L. Bodhe, B. Sellergren and Y. Anjaneyulu,  
509 *Environ. Sci. Technol.*, 2009, **43**, 2871-2877.
- 510 16. A. Rachkov, S. McNiven, A. El'skaya, K. Yano and I. Karube, *Anal. Chim. Acta*, 2000, **405**,  
511 23-29.
- 512 17. A. Valero-Navarro, A. Salinas-Castillo, J. F. Fernández-Sánchez, A. Segura-Carretero, R.  
513 Mallavia and A. Fernández-Gutiérrez, *Biosens. Bioelectron.*, 2009, **24**, 2305-2311.
- 514 18. H. Kubo, N. Yoshioka and T. Takeuchi, *Org. Lett.*, 2005, **7**, 359-362.
- 515 19. J. Matsui, H. Kubo and T. Takeuchi, *Anal. Chem.*, 2000, **72**, 3286-3290.
- 516 20. P. Turkewitsch, B. Wandelt, G. D. Darling and W. S. Powell, *Anal. Chem.*, 1998, **70**,  
517 2025-2030.

- 518 21. R. Challa, A. Ahuja, J. Ali and R. Khar, *Aaps Pharmscitech*, 2005, **6**, E329-E357.  
519 22. J. Szejtli, *Chem. Rev.*, 1998, **98**, 1743-1754.  
520 23. F. Hapiot, S. Tilloy and E. Monflier, *Chem. Rev.*, 2006, **106**, 767-781.  
521 24. K. A. Connors, *Chem. Rev.*, 1997, **97**, 1325-1358.  
522 25. Y. Yang, Y. Y. Long, Q. Cao, K. Li and F. Liu, *Anal. Chim. Acta*, 2008, **606**, 92-97.  
523 26. H. Asanuma, M. Kakazu, M. Shibata, T. Hishiya and M. Komiyama, *Supramol. Sci.*, 1998, **5**,  
524 417-421.  
525 27. T. Hishiya, M. Shibata, M. Kakazu, H. Asanuma and M. Komiyama, *Macromolecules*, 1999,  
526 **32**, 2265-2269.  
527 28. H. M. Liu, C. H. Liu, X. J. Yang, S. J. Zeng, Y. Q. Xiong and W. J. Xu, *Anal. Chim. Acta*, 2008,  
528 **628**, 87-94.  
529 29. H. A. Tsai and M. J. Syu, *Biomaterials*, 2005, **26**, 2759-2766.  
530 30. R. Y. Hsieh, H. A. Tsai and M. J. Syu, *Biomaterials*, 2006, **27**, 2083-2089.  
531 31. A. Bossi, F. Bonini, A. P. F. Turner and S. A. Piletsky, *Biosens. Bioelectron.*, 2007, **22**,  
532 1131-1137.  
533 32. Y. Cheng, P. Jiang, S. Lin, Y. N. Li and X. C. Dong, *Sensor. Actuat. B-Chem*, 2014, **193**,  
534 838-843.  
535 33. Y. Liu, J. Shi and D. S. Guo, *J Org Chem*, 2007, **72**, 8227-8234.  
536 34. H. G. Xie, P. F. Wang and S. K. Wu, *Prog. Nat. Sci.*, 2000, **10**, 27-32.  
537 35. Y. Liu, B. H. Han, B. Li, Y. M. Zhang, P. Zhao, Y. T. Chen, T. Wada and Y. Inoue, *J.*  
538 *Org. Chem.*, 1998, **63**, 1444-1454.  
539 36. G. C. Catena and F. V. Bright, *Anal. Chem.*, 1989, **61**, 905-909.  
540 37. J. A. Byun, S. H. Lee, B. H. Jung, M. H. Choi, M. H. Moon and B. C. Chung, *Biomed.*  
541 *Chromatogr.*, 2008, **22**, 73-80.  
542 38. A. A. Elbashir, S. Krieger and O. J. Schmitz, *Electrophoresis*, 2014, **35**, 570-576.  
543 39. D. Bartos, R. A. Campbell, F. Bartos and D. P. Grettie, *Cancer Res.*, 1975, **35**, 2056-2060.  
544  
545